# Exciton Diffusion in Conjugated Polymers: From Fundamental Understanding to Improvement in Photovoltaic Conversion Efficiency

Yasunari Tamai,[†] Hideo Ohkita,*,[†,‡] Hiroaki Benten,[†] and Shinzaburo Ito[†]

[†]Department of Polymer Chemistry, Graduate School of Engineering, Kyoto University, Katsura, Nishikyo, Kyoto 615-8510, Japan
[‡]Japan Science and Technology Agency (JST), PRESTO, 4-1-8 Honcho Kawaguchi, Saitama 332-0012, Japan

ABSTRACT: Singlet exciton diffusion plays a central role in the photovoltaic conversion in organic photovoltaics (OPVs). Upon light absorption, singlet excitons are promptly generated in organic materials instead of charge carriers because the dielectric constant (ε_r) is small (~3−4), which is in sharp contrast to inorganic and perovskite solar cells. In order to convert to charge carriers, excitons need to diffuse into an interface between electron donor and acceptor materials before deactivating to the ground state. Therefore, fundamental understanding of exciton diffusion dynamics is one of the most important issues to further improve OPVs. We highlight recent leading studies in this field and describe several approaches for efficient exciton harvesting at the interface in OPVs.
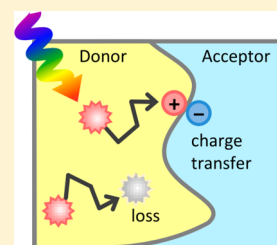
$\mathbf{S}$inglet excitons in organic materials are Coulombically bound electron−hole pairs, and hence cannot generate a photocurrent. For photovoltaic applications, electron donor/acceptor heterojunctions are used to generate charge carriers, at which excitons can be dissociated owing to the energy offset in the lowest unoccupied molecular orbital (LUMO) between donor and acceptor materials that is enough to break the Coulomb attraction.[1−10] Thus, excitons need to diffuse into the interface to convert to charge carriers before deactivating to the ground state. The exciton diffusion length L_D is a characteristic physical quantity, which is given by $L_D = (D\tau)^{1/2}$ where D is the diffusion coefficient and τ is the exciton lifetime. Since the lifetime of the singlet exciton in most conjugated polymer films is short, typically less than 1 ns, the diffusion lengths are limited to less than 20 nm, which is much shorter than the optical absorption pass length (~100−200 nm). Consequently, only a limited part of excitons can diffuse to the interface in planar heterojunction (PHJ) solar cells. As such, the bulk hetero-junction (BHJ) concept has been widely applied to organic photovoltaics (OPVs) in order to harvest many more excitons at the interface, in which excitons can easily arrive at the interface when the domain size of donor and acceptor materials is smaller than the diffusion length.[11,12] Conversely, domains of donor and acceptor materials that are too small are detrimental to efficient charge collection because of severe charge recombination.[13] We therefore should understand the exciton diffusion length to optimize the device morphology rationally.

Fundamental understanding of exciton diffusion dynamics in conjugated polymers have been addressed by many researchers. In one of the simplest cases, exciton diffusion can be considered to be a series of energy migration among identical chromophores. The energy migration takes place on the basis of either the Förster or Dexter mechanism.[14,15] The Förster mechanism is a long-range resonant energy transfer mediated by dipole−dipole interaction between the donor and acceptor.

In this model, the transfer rate is dependent on the oscillator strength of both donor and acceptor. On the other hand, the Dexter mechanism is known as a short-range energy transfer based on electron exchange, which requires spatial overlap of wave functions of the donor and acceptor. Thus, in singlet exciton diffusion, the Förster mechanism is much more important because of the long-range interaction. On the other hand, in the triplet exciton diffusion, the Dexter energy transfer is important because of the spin-forbidden transition between the ground and triplet states. Because of the long-range interaction in the Förster mechanism, the diffusion coefficient of singlet excitons is usually larger than that of triplet excitons. The conventional Förster formalism has been successfully applied to predict the diffusion length of small molecules.[16−18] On the other hand, because conjugated polymers are inherently inhomogeneous materials, diffusion dynamics is much more complicated in conjugated polymer films than in small molecules. In conjugated polymer films, exciton diffusion dynamics significantly depends on energetic, spatial, and orientational disorders as will be discussed later.

> Because conjugated polymers are inherently inhomogeneous materials, diffusion dynamics is much more complicated in conjugated polymer films than in small molecules.
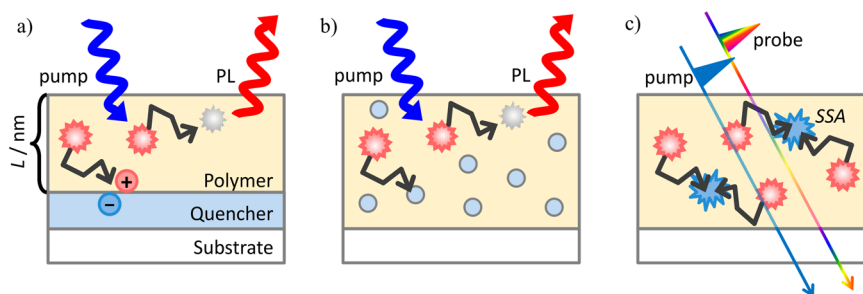
Figure 1. Schematic illustrations of (a) surface PL quenching method, (b) bulk PL quenching method, and (c) SSA analysis based on transient absorption spectroscopy.

To date, various spectroscopic techniques have been performed to observe the exciton diffusion dynamics, and those are basically categorized into two groups: (1) photoluminescence (PL) quenching based on exciton quenching molecules and (2) exciton self-quenching based on singlet–singlet exciton annihilation (SSA). Alternately, charge carrier techniques such as the photovoltaic response of solar cells and microwave conductivity measurements have also been performed to evaluate the diffusion length.[19,20] In this Perspective, we highlight recent efforts for in-depth understanding of exciton diffusion dynamics by spectroscopic techniques. In particular, we focus on the exciton diffusion dynamics in conjugated polymer films because excellent studies have already been published on small molecules.[15−18,21−24] We start with a brief introduction of two measuring techniques of the diffusion length L_D, namely, the PL quenching method and the SSA analysis. Then, we review recent findings on the exciton diffusion dynamics in conjugated polymer films. Finally, we give an outlook for further improvement in exciton harvesting efficiency at the interface in OPVs.

PL Quenching Method. One of the simplest methods for evaluating the L_D is the steady-state or time-resolved PL measurements in the absence and presence of exciton quenchers because these techniques do not need the high excitation intensity required for SSA measurements. The PL quenching efficiency Φ_q is evaluated as $\Phi_q = 1 - I/I_0 = 1 - \tau/\tau_0$ where I and τ (I_0 and τ_0) are the PL intensity and lifetime in the presence (absence) of exciton quenchers, respectively. The steady-state PL measurement is the easiest way for evaluating the Φ_q. However, this method is likely to suffer from relatively large experimental errors because the PL intensity is sensitively dependent on the optical geometry. On the other hand, the time-resolved PL measurement is independent of the optical geometry and, hence, exhibits a high reproducibility. However, prompt decay dynamics beyond temporal resolution cannot be detected. Thus, steady-state and time-resolved measurements should be performed complementary to confirm the consistency of the evaluated Φ_q.

As shown in Figure 1a and b, two typical sample structures are employed in these measurements. One is the bilayer film of conjugated polymers and exciton quenchers (the surface PL quenching method, Figure 1a).[25−33] The other is the polymer film mixed with a small amount of exciton quenchers (the bulk PL quenching method, Figure 1b).[34−36]

In the surface PL quenching method, the PL quenching efficiency of conjugated polymers is measured as a function of the polymer thickness L as shown in Figure 2. From the analysis of the thickness dependence of the PL quenching efficiency, the L_D can be evaluated. Because it can be safely
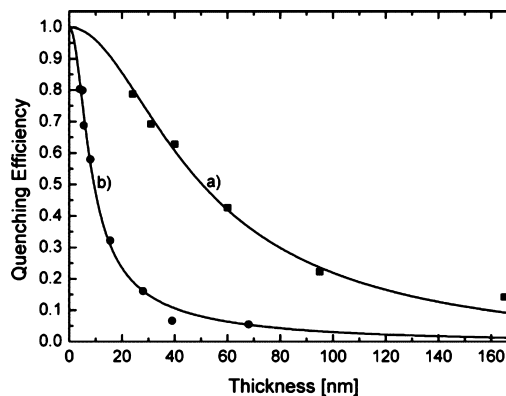
Figure 2. Relative PL quenching efficiency in (a) NRS-PPV/C$_{60}$ and (b) NRS-PPV/poly(F2D) heterostructures for different polymer film thickness. Reprinted from ref 25. Copyright 2005 American Chemical Society.

assumed that there is no gradient of exciton density in the direction parallel to the interface in the bilayer structures, the continuity equation for the exciton density is given by eq 1 as one-dimensional (1D) diffusion formula

$$\frac{\partial n(x, t)}{\partial t} = D\frac{\partial^2 n(x, t)}{\partial^2 x} - \frac{n(x, t)}{\tau} + G(x) \tag{1}$$

where $n(x,t)$ is the exciton density at a position x and time t, and $G(x)$ is the exciton generation rate at the position x. The first, second, and third terms of the right-hand side represent exciton diffusion, exciton deactivation via the radiative and nonradiative decays, and photon absorption with an absorption coefficient α, respectively. In eq 1, bimolecular exciton deactivation processes such as singlet–singlet, singlet–triplet, and singlet–polaron annihilations are assumed to be absent, which is appropriate when the pump intensity is weak enough. At the quenching interface, it is assumed that all the excitons arriving at the interface are quenched by the acceptor layer with an infinite charge transfer rate. At the nonquenching film/air interface, it is assumed that excitons are reflected without any quenching. These boundary conditions are given by

$$n|_{\text{quench}} = 0 \tag{2}$$

$$\frac{\partial n}{\partial x}\bigg|_{\text{nonquench}} = 0 \tag{3}$$

for the quenching and nonquenching interfaces, respectively. Eq 1 can be solved under the boundary conditions of eqs 2 and 3. As a result, the quenching efficiency Φ_q is calculated as a

function of polymer thickness L as well as the diffusion length L_D and the absorption coefficient α as follows[25,26]

$$\Phi_q(L, L_D, \alpha) = 1 - \frac{\int_0^\infty \int_0^L n(x, t, L_D, \alpha) \mathrm{d}x\mathrm{d}t}{\int_0^\infty \int_0^L n_{ref}(x, t, L_D) \mathrm{d}x\mathrm{d}t}$$

$$= \frac{[\alpha^2 L_D^2 + \alpha L_D \tanh(L/L_D)]\exp(-\alpha L) - \alpha^2 L_D^2[\cosh(L/L_D)]^{-1}}{(1 - \alpha^2 L_D^2)[1 - \exp(-\alpha L)]}$$

(4)

where n and n_{ref} are the exciton density with and without the quenching layer, respectively. Under the uniform excitation condition across optically thin films, eq 4 can be simplified as

$$\Phi_q(L, L_D) = \frac{L_D}{L}\tanh\left(\frac{L}{L_D}\right)$$

(5)

We note that a flat and smooth interface is highly required for accurate evaluation of the L_D because the exciton diffusion and subsequent charge transfer occur only in the limited distance typically as short as ~10 and ~1 nm, respectively, from the interface. Fullerene and its soluble derivatives such as [6,6]-phenyl-C_{61}-butyric acid methyl ester (PCBM) are the most reliable exction quenching acceptors for OPVs. Thus, fullerenes have been employed as the quenching layer in bilayer films for the surface PL quenching measurements. However, recent studies have shown that low-molecular-weight fullerenes are likely to diffuse into the polymer layers even at room temperature,[37,38] resulting in collapse of the well-defined bilayer structure and overestimation of the diffusion length as shown in Figure 2.[25] To overcome the interdiffusion of fullerenes into the polymer layer, various cross-linkable derivatives have been synthesized and used to fabricate well-defined layered structures.[25,30,33]

As an alternative to the surface quenching in bilayer films, the bulk PL quenching method has also been employed to examine the exciton diffusion. In this method, a small amount of exciton quenchers such as fullerenes are dispersed homogeneously in polymer films, and the PL quenching efficiencies of conjugated polymers are measured as a function of quencher concentration as shown in Figure 3. The PL quenching efficiency is then analyzed by a Monte Carlo simulation or by the Stern–Volmer formalism eq 6
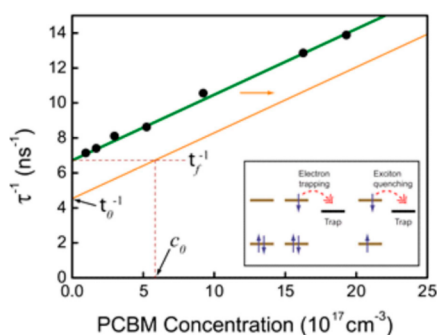
Figure 3. Stern–Volmer plots of PCPDTBT:PCBM blends. The inset is a schematic representation of the electron transfer process from polymer to the defect state for the case of electron trapping and exciton quenching. Reprinted with permission from ref 35. Copyright 2013 WILEY-VCH Verlag Gmbh & Co. KGaA, Weinheim.

$$\frac{1}{\tau} = \frac{1}{\tau_0} + 4\pi DR[Q]$$

(6)

where R is the effective exciton quenching radius, and $[Q]$ is the quencher concentration. The limitation of this technique would arise from difficulty of dispersing quenchers into thin films homogeneously and the uncertainty of estimating the minute quencher concentration $[Q]$ accurately, both of which would be difficult if polymers or quenchers easily form aggregates in films. The same is true for the Monte Carlo simulation.

Singlet–Singlet Exciton Annihilation. The exciton diffusion dynamics can also be discussed by analyzing exciton self-quenching dynamics due to SSA.[32,39–41] In this method, exciton quenchers, which may disturb polymer morphology, are not necessary. Instead, high excitation intensity is required to induce SSA (Figure 1c), which may also induce other nonlinear phenomena. At higher excitation intensities, the exciton decay becomes more rapid at a shorter time stage but independent of the intensity at a longer time stage. The faster decay is dependent on the excitation intensity, suggesting higher order reactions most probably due to SSA. The slower decay that is independent of the intensity is attributable to intrinsic exciton lifetime due to the radiative and nonradiative deactivations of singlet excitons. The rate equation for the singlet exciton decay is given by

$$\frac{\mathrm{d}N(t)}{\mathrm{d}t} = -\frac{N(t)}{\tau} - \frac{1}{2}\gamma(t)N(t)^2$$

(7)

where $N(t)$ is the exciton density at a delay time t after the laser excitation, and $\gamma(t)$ is the bimolecular decay rate coefficient for SSA. The factor 1/2 represents that only one exciton is left after SSA ($S_1 + S_1 \rightarrow S_n + S_0 \rightarrow S_1 + S_0 + phonon$). Eq 7 is solved as follows

$$N(t) = \frac{N_0\exp(-t/\tau)}{1 + \frac{1}{2}N_0\int_0^t \gamma(t')\exp(-t'/\tau)\mathrm{d}t'}$$

(8)

Because SSA in conjugated polymer films is usually a diffusion limited process, the annihilation rate coefficient $\gamma(t)$ is a function of diffusion coefficient. In other words, diffusion parameters can be evaluated from the annihilation rate coefficient $\gamma(t)$, which can be directly extracted from experimental decay curve by introducing a new variable eq 9

$$Y(t) = \exp(-t/\tau)N(t)^{-1}$$

(9)

By substituting eq 7 into eq 9, a linearized differential equation is obtained

$$\frac{\mathrm{d}Y(t)}{\mathrm{d}t} = \frac{1}{2}\gamma(t)\exp(-t/\tau)$$

(10)

Thus, the time dependence of the annihilation rate coefficient can be directly extracted from two observables: intrinsic exciton lifetime and exciton density.

As discussed previously, the diffusion-limited bimolecular reaction rates significantly depend on the dimensionality of the system.[40–43] In the 3D diffusion, $\gamma(t)$ is given by eq 11

$$\gamma_{3D}(t) = 8\pi DR\left(1 + \frac{R}{\sqrt{2\pi Dt}}\right)$$

(11)

where R is the effective interaction radius of singlet excitons. For a later time stage ($t \gg R^2/(2\pi D)$), the annihilation rate

coefficient can be expressed as the time-independent formula $\gamma_{3D} = 8\pi DR$. In the 2D diffusion, $\gamma(t)$ is given by eq 12

$$\gamma_{2D}(t) = \frac{8DR}{\pi} \int_0^\infty \frac{\exp(-Du^2 t)}{u[J_0^2(uR) + Y_0^2(uR)]} du \qquad (12)$$

where J_0 and Y_0 are zero order Bessel functions of the first and second kind, respectively. In the 1D diffusion, $\gamma(t)$ is given by eq 13

$$\gamma_{1D}(t) = 4\pi DR \frac{R}{\sqrt{2\pi Dt}} \qquad (13)$$

In summary, the bimolecular rate coefficient becomes time-independent in the 3D system and $t^{-\alpha}$ ($\alpha < 1/2$) dependent in the 2D system at larger t, and is consistently $t^{-1/2}$ dependent in the 1D system over the whole time domain (details are summarized in refs 40 and 41). Thus, we can discuss not only the diffusion length but also the dimensionality of the exciton diffusion dynamics on the basis of the time dependence of the annihilation rate coefficient.

Exciton Diffusion Dynamics. The exciton diffusion dynamics has been evaluated for a variety of conjugated polymers by the PL quenching methods. Among them, a prototypical conjugated polymer poly(*p*-phenylene vinylene) (PPV) and its derivatives have been most widely studied. The diffusion lengths have been reported to be 5−7 nm.[25−29,44] Table 1 summarizes the L_D reported for various amorphous polymer films evaluated by the PL quenching methods.

Table 1. Exciton Diffusion Length Reported for Various Amorphous Polymers

polymer	method (quencher)[a]	L_D/nm	reference number
NRS-PPV	SQ (PF2D)	5 ± 1	25
NRS-PPV	SQ (PF2D)	6	26
MEH-PPV		7	
BEH-PPV		6.5	
NRS-PPV	SQ (PF2D)	7	27
MDMO-PPV	SQ (TiO₂)	6 ± 1	28
MDMO-PPV	SQ (PF2D)	4.5 (293 K)	29
PF12TBT	SQ (*p*-PCBVB)	11	33
PCPDTBT	BQ (PCBM)	10.6 ± 0.6	34
NRS-PPV	BQ (PCBM)	~ 3.5	35
MEH-PPV		~ 7	
PCPDTBT		~ 6	
F8BT		~ 8	
TFB	BQ (various fullerene derivatives)	9.0 ± 2	36

^{a}SQ: surface PL quenching. BQ: bulk PL quenching.

As mentioned above, inhomogeneity in conjugated polymers plays a central role in the exciton diffusion dynamics. Mikhnenko et al. have reported temperature dependence of the exciton diffusion in MDMO-PPV, for which they observed that both L_D and D decrease with decreasing temperature.[29] They found that there are two regimes in the exciton diffusion at room temperature: initial temperature-independent migration, followed by thermally activated diffusion, the latter of which is switched off below ~150 K. Owing to disorder in conjugated polymer films, the density of states (DOS) is widely distributed in energy. Excitons, therefore, migrate toward sites

of lower energy on a time scale of pico- to nanoseconds, which is called downhill energy relaxation as schematically shown in Figure 4.[29,39,41,45,46] After reaching thermal equilibrium,
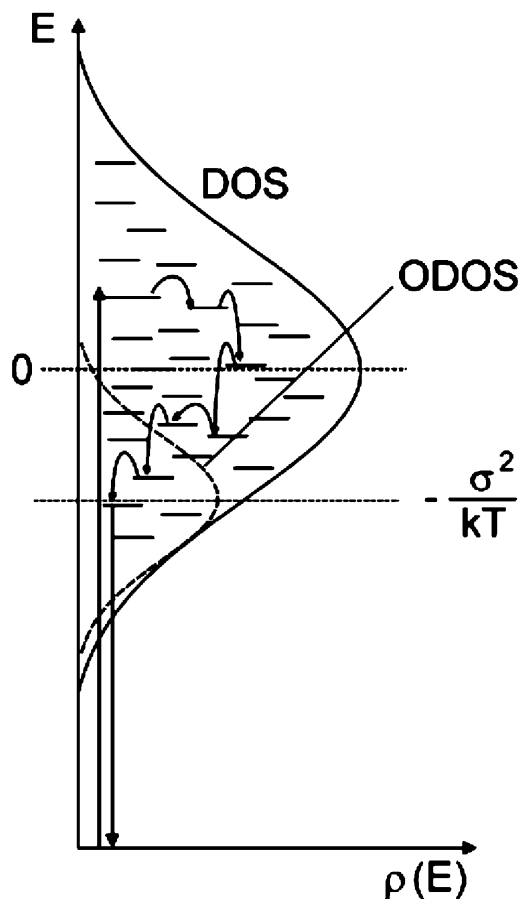
Figure 4. Gaussian DOS in disordered materials. After photoexcitation into upper states the exciton tends to relax to sites of lower energy in the tail of the DOS and finally diffuses around its equilibrium energy. The equilibrium energy is offset by $-\sigma^2/kT$ with respect to the center of the DOS. Reprinted with permission from ref 45. Copyright 2009 WILEY-VCH Verlag Gmbh & Co. KGaA, Weinheim.

excitons then migrate through thermally activated hopping. The initial downhill migration would be much faster than the later thermally activated hopping per one step owing to its exothermicity. On the other hand, the time scale of the downhill relaxation is much shorter than that of the thermally activated hopping regime. As such, the diffusion length at room temperature would be limited by the slow thermally activated hopping rather than the rapid downhill migration.

Markov et al. have studied the exciton diffusion anisotropy of the NRS-PPV polymer layer with a thickness of less than 10 nm by the time-resolved surface PL quenching.[27] They found that, in such an ultrathin film, conjugated polymer main chains are mostly aligned in the plane of the quenching layer, and excitons diffuse preferentially in the direction perpendicular to the surface, suggesting that interchain exciton hopping is much faster than intrachain hopping. Similar conclusions have been reported by other research groups.[47−49] Beljonne et al. assessed both inter- and intrachain exciton diffusion processes experimentally and theoretically in a polyindenofluorene with a perylene derivative attached to the chain ends (PEC-PIFTEH).[47] From the time-resolved PL measurements in

both solution and film, they found that PL of polyindeno-fluorene was quenched by the perylene derivative much faster in film than in solution, suggesting that interchain exciton hopping is faster than intrachain hopping. Quantum chemical calculations complement their observations that the interchain electronic couplings and the corresponding transfer rates are always larger than the corresponding intrachain ones, suggesting that close contact between cofacially aligned chromophores provide an efficient pathway for energy migration due to the stronger exciton coupling. It should be noted, however, that they also pointed out that the intrachain migration would be much faster if the chains were perfectly conjugated and excitations could move coherently along the chains.

As such, we can easily expect that the exciton diffusion dynamics is more complicated in crystalline polymers than in amorphous polymers. We should keep in mind that deeper understanding of exciton diffusion dynamics in crystalline polymers would be difficult by the PL quenching techniques because spatial and temporal distribution of exciton diffusivity is averaged in these techniques. For example, although there is good agreement in the L_D in PPVs as reported previously, there is a significant discrepancy in the L_D reported for regioregular poly(3-hexylthiophene) (RR-P3HT) crystalline films from 2.7 to 27 nm.[30−32,35,39,41,50,51] It has been reported to be typically <10 nm on the basis of the PL quenching methods[30−32,35,50,51] and >10 nm on the basis of the SSA analysis.[39,41] This is probably because homogeneous exciton diffusion is typically assumed in the analytical diffusion models described above, which is likely not the case for RR-P3HT. Crystalline polymers like RR-P3HT generally consist of not only crystalline but also amorphous domains with different ratios depending on fabrication conditions. As a result, the diffusion length evaluated by the PL quenching would be the average of crystalline and amorphous domains because the conjugated polymer layer should have both domains. Furthermore, the time-dependence of SSA in RR-P3HT crystalline films has been still a controversial issue: both time-independent[32] and time-dependent[39] SSAs have been reported. In ref 32, the time-resolved PL measurements were performed with an excitation wavelength of 400 nm. The SSA dynamics was analyzed by using time-independent formula and was attributed to isotropic exciton diffusion. On the other hand, the t^{-1} dependence of the annihilation rate coefficient has been reported in ref 39 by the time-resolved PL measurements with an excitation wavelength of 532 nm. As is discussed in the literature, the t^{-1} dependence is attributed to downhill relaxation in the DoS in P3HT films.

> One reason for the discrepant statements in previous reports is probably because the inherent exciton dynamics in crystalline domains would be masked by exciton dynamics in disordered amorphous domains.

One reason for the discrepant statements in previous reports is probably because the inherent exciton dynamics in crystalline domains would be masked by exciton dynamics in disordered amorphous domains. Recently, the exciton diffusion dynamics in RR-P3HT crystalline domains has been carefully studied by

analyzing SSA on the basis of transient absorption measurements.[41] The crystalline domains were selectively excited at an absorption band-edge of RR-P3HT at 620 nm where the absorption is safely ascribed to crystalline domains,[52−54] which is in sharp contrast to previous studies. Upon selective excitation of crystalline P3HT at an absorption edge of 620 nm, no peak shift of the singlet exciton absorption band was observed, suggesting singlet exciton dynamics in relatively homogeneous P3HT crystalline domains without downhill relaxation in the DoS. This finding is in a sharp contrast to the exciton dynamics upon the selective excitation of amorphous domains at 400 nm where the downhill relaxation was observed.

Even under such crystalline selective excitation conditions, the annihilation rate coefficient was still dependent on time: $\gamma(t) \propto t^{-1/2}$ as shown in Figure 5. The $t^{-1/2}$ dependence is not
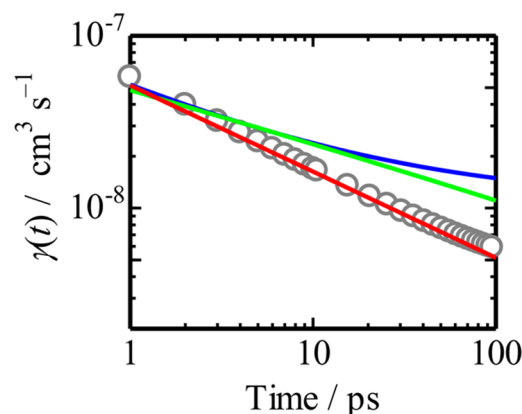
Figure 5. Annihilation rate coefficient for a P3HT film excited at 620 nm extracted from eq 10. The red line represents the fitting curve using the 1D model (eq 13). The blue and green lines represent the annihilation rate coefficient calculated by the 3D and 2D models (eqs 11 and 12, respectively). Adapted from ref 41. Copyright 2014 American Chemical Society.

ascribed to the downhill relaxation in the DoS because no spectral shift is observed by the laser excitation at the absorption edge of crystalline P3HT, but rather it can be ascribed to inherent exciton dynamics in P3HT crystalline domains.

As shown in Figure 5, the time dependence of the extracted annihilation rate coefficient is best fitted with the 1D exciton diffusion model over a wide temporal range. In contrast, there is a considerable discrepancy both in the 2D and 3D exciton diffusion models: they deviate from the $t^{-1/2}$ dependence in a longer time region. Therefore, the $t^{-1/2}$ dependence is attributed to the 1D exciton diffusion. This is probably because RR-P3HT self-organizes 1D fibrils consisting of π-stacking lamellae,[55−57] and consequently the interchain exciton coupling is larger than the intrachain coupling as is predicted theoretically.[58]

As summarized in Table 2, D and L_D increase with increasing crystallinity.[10] The diffusion length L_D in the highly crystalline RR-P3HT film is as long as 20 nm, which is about four times longer than that in the amorphous regiorandom P3HT (RRa-P3HT) film. This strong crystallinity dependence of the L_D would be the origin of the large discrepancy in the L_D reported for RR-P3HT previously. These experimental results agree very well with recent calculations.[59−62] From the dependence of Stokes shift on the number of chromophores in the H-

Table 2. Diffusion Parameters of Singlet Excitons in P3HT Films with Different Crystallinity

samples[a]	$D/10^{-3}$ cm^2 s^{-1}	L_D/nm	dimension
RR-P3HT-H	7.9	20	1D
RR-P3HT-L	3.3	14	1D
RRa-P3HT	0.46	4.8	3D

[a]RR-P3HT-H: high-crystallinity P3HT. RR-P3HT-L: low-crystallinity P3HT.

Figure 6. PL efficiencies for the DPP-based polymer/PC$_{71}$BM blends normalized to the PL intensities of the pure films. The solid symbols show the polymer PL under excitation at 790 nm and the open symbols show the PC$_{71}$BM PL under excitation at 532 nm. For all measurements, the PL was integrated over the entire emission spectra. Reproduced from ref 74 with permission from the PCCP Owner Societies.

aggregate model, Spano et al. estimated the diffusion length to be 15 nm for a P3HT film.[59] Köse et al. performed kinetic Monte Carlo simulation with a combination of time-dependent density functional theory (TDDFT) and molecular dynamics (MD) calculations and estimated the L_D in crystalline and amorphous P3HT domains to be ~20 and 5.7 nm, respectively.[61,62] We therefore emphasize that ultrafast transient spectroscopy by the selective excitation is of particular importance for studying exciton diffusion dynamics in crystalline domains.

Relevance to OPVs and Outlook. In amorphous or less crystalline polymers blended with PCBM such as RRa-P3HT and poly[[4,4-bis(2-ethylhexyl)-4H-cyclopenta[2,1-b;3,4-b′]-dithiophene)-2,6-diyl-*alt*-(2,1,3-benzothiadiazole)-4,7-diyl] (PCPDTBT), singlet excitons rapidly convert into polarons within a picosecond after the light absorption, indicating that the polymer and PCBM are mixed well with each other. In other words, the exciton harvesting efficiency is almost 100% for amorphous polymer blends.[63−65] Rather, such amorphous polymer solar cells suffer from the lower fill factor (FF) for the thicker active layer because of severe nongeminate charge recombination.[64,66] As a result, the power conversion efficiency (PCE) is typically optimized with optically thin (~100 nm) films. On the other hand, several highly crystalline polymers such as RR-P3HT have shown high fill factors with thick (>200 nm) active layers,[66−70] suggesting that highly crystalline polymers have a potential advantage for high-performance OPVs. Although the exciton harvesting efficiency is as high as ~85−90%, this is one of the largest bottlenecks in such highly crystalline polymer solar cells.[63,65,71] In other words, more than 10% excitons are lost because of relatively large crystalline domains in the blend film. More serious cases have been reported for highly crystalline polymer solar cells.[72−74] For example, as shown in Figure 6, more than half of the polymer excitons are lost in a highly crystalline diketopyrrolopyrrole (DPP)-based polymer blended with [6,6]-phenyl-C$_{71}$-butyric acid methyl ester (PC$_{71}$BM).[74] This is due to a large domain size and a short exciton diffusion length of the DPP-based polymer. In summary, highly crystalline polymer solar cells have the potential to achieve a good balance between high FF and the optically thick active layer to absorb the solar light thoroughly, but they are likely to suffer from relatively low exciton harvesting efficiency. Therefore, the key challenging issue is to achieve a high exciton harvesting efficiency in highly crystalline polymer solar cells, which are the most likely candidates for further improvement in the PCE toward 15%.

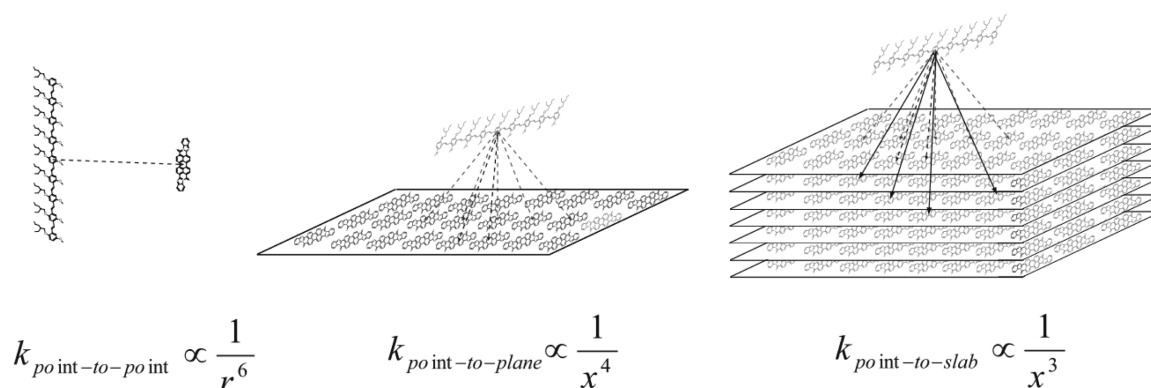Exciton harvesting efficiency at the interface η_{ED} is roughly given by

$$\eta_{ED} = 1 - \frac{\tau}{\tau_0} = 1 - \frac{L^2}{L_D^2} \qquad (14)$$

> Highly crystalline polymer solar cells have the potential to achieve a good balance between high FF and the optically thick active layer to absorb the solar light thoroughly, but they are likely to suffer from relatively low exciton harvesting efficiency. Therefore, the key challenging issue is to achieve a high exciton harvesting efficiency in highly crystalline polymer solar cells, which are the most likely candidates for further improvement in the PCE toward 15%.

where τ and τ_0 are exciton lifetime of the blend and neat polymer films, respectively, and L is the exciton travel distance in the duration τ. In other words, L corresponds to half the domain size. Decreasing L would result in higher η_{ED} but also would promote charge recombination as mentioned above. In order to harvest all the excitons without charge recombination loss, therefore, the exciton diffusion length should be lengthened. According to the rough estimation, an L_D of ~50 nm would be necessary to harvest almost all the excitons with a domain size of $2L \sim 20$ nm. To the best of our knowledge, such long diffusion lengths have never been reported for conjugated polymers, but there are many reports for small molecule crystals.[15,21,40,75−77] For example, diffusion lengths of ~100 nm have been reported for anthracene single crystals, suggesting that there is still room to lengthen the L_D of conjugated polymers. The longer diffusion lengths in molecular crystals are mainly attributed to the higher structural order and smaller trap density of the crystal. Recent theoretical studies have shown that a coherent length of the RR-P3HT exciton along π-stacks is estimated to be only ~2 or 3 stacks,[59,78] suggesting there are significant disorders even in RR-P3HT crystalline domains. For further improvements in the diffusion length, therefore, it

$$k_{point-to-point} \propto \frac{1}{r^6} \qquad k_{point-to-plane} \propto \frac{1}{x^4} \qquad k_{point-to-slab} \propto \frac{1}{x^3}$$

Figure 7. Schematics showing representations of three different geometries for energy transfer, point-to-point (left), point-to-plane (center), and point-to-slab (right). For simplicity, only the excited chromophore is drawn on the donor side, whereas in physically relevant systems the excited chromophore is embedded in a 3D matrix of nonexcited donor chromophores. Small D−A separation distance were chosen to emphasize the various possible transfer pathways. At larger distance (>10 nm), the donor would look like a point and the acceptor planes and slabs would appear to be continuous. The arrows show representative energy transfer pathways. Point-to-point corresponds to the situation where both donor and acceptor chromophores are randomly dispersed in a matrix. In the limit that acceptor film thickness l is much less than the donor−acceptor separation distance ($l/r \ll 1$), a donor chromophore can couple to a 2D sheet of acceptor molecules (point-to-plane). In the limit where l is relatively thick, a donor chromophore can couple to a 3D array of acceptor molecules (point-to-slab). Reprinted with permission from ref [81]. Copyright 2007 WILEY-VCH Verlag Gmbh & Co. KGaA, Weinheim.

would be of utmost importance to increase crystalline order. In practical cases, however, we cannot always obtain higher crystallinity in OPVs without any changes in other parameters such as domain size. Herein, we therefore describe two alternative methodologies to improve exciton harvesting efficiency.

Exciton Harvesting through Förster Energy Transfer. Förster energy transfer between different materials would enhance the exciton diffusion because the energy transfer distance is typically longer than the energy migration distance per one step. Assuming point-dipoles, the rate coefficient of Förster energy transfer k_F between two chromophores is proportional to $1/r^6$ as

$$k_F(r) = \frac{1}{\tau}\left(\frac{R_0}{r}\right)^6 \tag{15}$$

where r is donor−acceptor separation distance and R_0 is the Förster radius. On the other hand, because the exciton in the donor can be transferred to any one of the acceptor chromophores, the total rate of Förster energy transfer is a sum over all possible transfer events. The rate from one donor to a 2D sheet is proportional to $1/r^4$ and to a 3D slab to $1/r^3$ as shown in Figure 7,[79−82] indicating that energy transfer to aggregates is much more efficient than to isolated chromophore.

We herein describe how effective the Förster energy transfer is in improving exciton harvesting efficiency. Eq 16 is a modified continuity equation of eq 1, which includes an additional term corresponding to exciton harvesting to the interface by Förster energy transfer with a rate coefficient k_F

$$\frac{\partial n(x,t)}{\partial t} = D\frac{\partial^2 n(x,t)}{\partial^2 x} - \frac{n(x,t)}{\tau} - k_F(x)n(x,t) + G(x) \tag{16}$$

$$k_F(x) = \frac{C_A}{\tau}\left(\frac{\pi}{6}\right)\frac{R_0^6}{(L-x)^3} \tag{17}$$

where point-to-slab (3D) model is applied with an acceptor chromophore density C_A. Solving eq 16 numerically under the same boundary conditions as eqs 2 and 3, the thickness dependence of exciton quenching efficiency is calculated as shown in Figure 8. In this simulation, the intrinsic diffusion
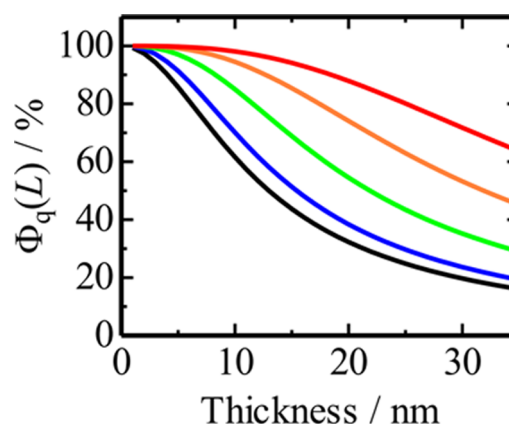

Figure 8. Simulated thickness dependence of the quenching efficiencies for diffusion-only (L_D = 7 nm, black) as well as diffusion and energy transfer with Förster radii of 2 nm (blue), 3 nm (green), 4 nm (orange), and 5 nm (red).

length of the donor material and acceptor chromophore density is fixed to 7 nm and 1.4 nm^{-3},[28] respectively. Apparent improvement in the quenching efficiency is observed with a Förster radius R_0 of >3 nm. When R_0 is 5 nm (red), the quenching efficiency is almost unity at L = 10 nm, and still ~90% at L = 20 nm.

> For further improvements in the diffusion length, therefore, it would be of utmost importance to increase crystalline order.

McGehee et al. performed a demonstrative experiment in which they used a highly efficient red emitting polymer DOW Red as the energy donor and a highly absorptive low-bandgap polymer PTPTB as the energy acceptor.[81] They estimated an intrinsic diffusion length of DOW Red to be 3 nm from PL quenching measurements of DOW Red on TiO_2, and an effective diffusion length of 27 nm in DOW Red/PTPTB bilayer films with a Förster radius R_0 of 3.7 nm.

This concept has been applied to bulk heterojunction OPVs by incorporating silicon phthalocyanine derivatives (SiPcs) into RR-P3HT/PCBM blends.[83−87] The third component dyes are likely to segregate at the interface as shown in Figure 9a
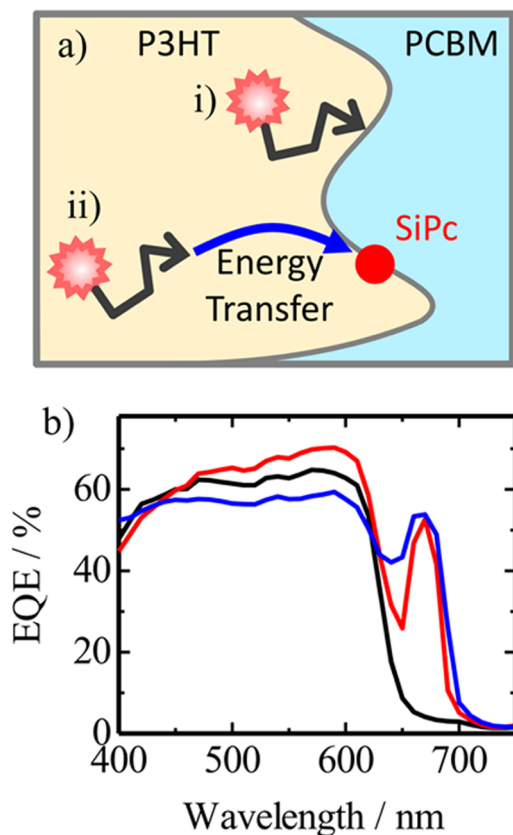
Figure 9. Schematic phase-separated morphology of P3HT/PCBM/SiPc ternary blend film. The third component dyes (red circle) are likely to segregate at the interface. In the absence of the dye (i), only excitons generated at nearby sites can reach the interface because the domain size is large. In the presence of the dye (ii), even excitons generated far away can reach the interface through energy transfer to the dye, followed by charge transfer to PCBM. (b) EQE spectra of RR-P3HT:PCBM:SiPc ternary blend with 4.8 wt % SiPc (red) and 17 wt % SiPc (blue) and RR-P3HT:PCBM (1:1) binary blend solar cells (black) after solvent annealing. Adapted with permission from ref 84. Copyright 2011 WILEY-VCH Verlag Gmbh & Co. KGaA, Weinheim.

because of the following two driving forces: (1) crystallization/aggregation of P3HT and PCBM and (2) surface free energy difference among those three materials. As a result, P3HT excitons are more effectively harvested at the interface through the energy transfer from P3HT to SiPc, followed by charge transfer to PCBM, resulting in the improvement in photovoltaic conversion efficiency of OPVs. This is clearly found in the external quantum efficiency (EQE) spectra of the ternary blend cell as shown in Figure 9b. At a dye concentration of 4.8 wt % (red line), EQE increased not only at the dye absorption

band at around 670 nm but also at the P3HT absorption band at 400−600 nm, which is attributed to efficient exciton harvesting through the energy transfer. The potential advantage of dye loading for exciton harvesting was limited because a large dye loading fraction is detrimental to charge collection as is discussed in ref 84. Very recently, a heterostructured dye SiPcBz6 has been synthesized and successfully applied for ternary OPVs.[87] The heterostructured SiPcBz6 is suitable for the selective loading to the interface with high dye concentrations and hence can boost the photovoltaic performance by ~30%. As an alternative ternary blend OPVs, Brabec et al. reported that the photocurrent is also increased by incorporating a low-bandgap donor polymer PSBTBT into RR-P3HT/PCBM blend cell.[88] In ref 82, it was found that the energy transfer from RR-P3HT to PSBTBT potentially enhances the effective diffusion length of RR-P3HT up to 30 nm in such ternary blends.[82]

Spin Conversion via Singlet Fission. Another way for improving the L_D is utilization of triplet excitons. Owing to their longer exciton lifetime up to milliseconds, the diffusion length of triplet excitons would be potentially longer than that of singlet excitons even though the diffusion coefficient is smaller than that of singlet excitons.[89−93] To date, triplet exciton diffusion length up to μm order has been reported for some molecular crystals.[93] The potential advantage of triplet exciton diffusion is also true for conjugated polymers. For example, Friend et al. reported that the triplet exciton diffusion length of F8BT is ~180 nm,[91] which is much longer than a singlet diffusion length of ~8 nm.[35]

Spin conversion from singlet to triplet state is generally forbidden because of the transition between different spin multiplicities. Indeed, intersystem crossing from singlet to triplet excitons proceeds on a time scale of nanoseconds in conjugated polymers[94] and, hence, not relating to the exciton harvesting process in OPVs. On the other hand, singlet fission from one singlet into two triplets is spin-allowed, in which one singlet exciton sharing its excitation energy with a neighboring ground state is converted into two triplet excitons.[95,96] Singlet fission is a multiple exciton generation process and, hence, has recently attracted much attention because it could potentially improve the photovoltaic efficiency beyond the Shockley−Queisser limit.[97,98] Although recent studies on singlet fission have focused on acene crystals such as pentacene and rubrene,[99−102] singlet fission in conjugated polymers has also been reported by several groups including ours.[103−108] Recently, fission efficiency of ~170% has been observed in a donor−acceptor type low-bandgap polymer.[108] Since the triplets energy generated by singlet fission is less than half the singlet energy, we face the difficulty in material and device designs when applying singlet fission into OPVs. This is one of the reasons why fission-based OPVs are far behind in the PCE to date. However, a breakthrough in this field would make singlet fission in conjugated polymers attract much more attention increasingly over the next several years.

In this Perspective, we have reviewed exciton diffusion dynamics in polymer thin films and exciton harvesting efficiency in OPVs. Through the discussion, a key determinant of the exciton diffusion dynamics is the spatial and energetic inhomogeneity, which intrinsically exists in conjugated polymers. In order to increase the diffusion length, therefore, decreasing disorder would be of utmost importance. Förster energy transfer and spin conversion into triplets through singlet fission would be promising candidates for further improvement

of the diffusion length. On the other hand, few studies of exciton diffusion dynamics for low-bandgap polymers used in state-of-the-art OPVs have been reported to date, and hence, exciton diffusion dynamics in novel low-bandgap polymers is still not clear. Although the low-bandgap polymers can absorb much more sunlight, lowering the bandgap also has a detrimental effect for exciton harvesting at the interface. According to the energy gap law, the nonradiative decay rate increases exponentially with a reduction of the bandgap. As a consequence of lowering the bandgap, the exciton lifetime of most low-bandgap polymers would be shortened compared with that of prototypical ones, resulting in a critical factor for shortening the diffusion length.[74] Further experimental and theoretical studies are needed for this important issue to improve the PCE.

AUTHOR INFORMATION

Corresponding Author
*E-mail: ohkita@photo.polym.kyoto-u.ac.jp.

Notes
The authors declare no competing financial interest.
All authors can be found in http://www.photo.polym.kyoto-u.ac.jp/en/members.

Biographies
Yasunari Tamai is a Postdoctoral Fellow in the Department of Polymer Chemistry at Kyoto University. He received his Doctoral degree from Kyoto University in 2013. He worked as a Research Fellow of Japan Society for the Promotion of Science (JSPS) from 2010 to 2013. His research interests include exciton and charge dynamics in polymer systems. His current research focuses on studying photovoltaic conversion mechanisms in polymer solar cells.

Hideo Ohkita is an Associate Professor in the Department of Polymer Chemistry at Kyoto University and concurrently a PRESTO researcher, Japan Science and Technology Agency (JST). He obtained a Doctoral degree in 1997 at Kyoto University. He became Assistant Professor in 1997 and was promoted to Associated Professor in 2006. He worked as an academic visitor with Professor Durrant at Imperial College London from 2005 to 2006. His research interests include studying photophysics and photochemistry in polymer systems. His current research focuses on spectroscopic approach to polymer solar cells.

Hiroaki Benten is an Assistant Professor in the Department of Polymer Chemistry at Kyoto University. He obtained a Doctoral degree in 2005 at Kyoto University. He worked as a JSPS postdoctoral fellow at Max-Planck Institute for Polymer Research (Mainz) in the laboratory of Professor Knoll from 2006 to 2008. He became Assistant Professor in 2008. He worked as an academic visitor with Professor Ginger at University of Washington in 2013. His current research interest is in the relationship between nanoscale morphology and device performance of polymer-based solar cells.

Shinzaburo Ito is a Professor in the Department of Polymer Chemistry at Kyoto University. He obtained his doctoral degree of Engineering in 1981 from Kyoto University. He was appointed as a Research Instructor of Kyoto University in 1979. He experienced being a guest scientist of Max Planck Institute for Polymer Research (Mainz) in the laboratory of Professor Knoll from 1991 to 1992 and was also a visiting research fellow of RIKEN (Wako) from 1993 to 1999. He was promoted to Associate Professor in 1994 and to Professor of Department of Polymer Chemistry, Kyoto University, in 1999. His research interests encompass the polymer nanostructure, polymer photophysics and photochemistry, ultrathin films, and their optical and electrical properties.

ACKNOWLEDGMENTS

REFERENCES

(1) Kippelen, B.; Brédas, J.-L. Organic Photovoltaics. *Energy Environ. Sci.* **2009**, *2*, 251−261.

(2) Deibel, C.; Dyakonov, V. Polymer−Fullerene Bulk Hetero-junction Solar Cells. *Rep. Prog. Phys.* **2010**, *73*, 096401.

(3) Clarke, T. M.; Durrant, J. R. Charge Photogeneration in Organic Solar Cells. *Chem. Rev.* **2010**, *110*, 6736−6767.

(4) Ohkita, H.; Ito, S. Transient Absorption Spectroscopy of Polymer-Based Thin-Film Solar Cells. *Polymer* **2011**, *52*, 4397−4417.

(5) Baranovskii, S. D.; Wiemer, M.; Nenashev, A. V.; Jansson, F.; Gebhard, F. Calculating the Efficiency of Exciton Dissociation at the Interface between a Conjugated Polymer and an Electron Acceptor. *J. Phys. Chem. Lett.* **2012**, *3*, 1214−1221.

(6) Ohkita, H.; Ito, S. Exciton and Charge Dynamics in Polymer Solar Cells. In *Organic Solar Cells*; Springer−Verlag: London, U.K., 2013.

(7) Dou, L.; You, J.; Hong, Z.; Xu, Z.; Li, G.; Street, R. A.; Yang, Y. 25th Anniversary Article: A Decade of Organic/Polymereric Photovoltaic Research. *Adv. Mater.* **2013**, *25*, 6642−6671.

(8) Dimitrov, S. D.; Durrant, J. R. Materials Design Considerations for Charge Generation in Organic Solar Cells. *Chem. Mater.* **2014**, *26*, 616−630.

(9) Gao, F.; Inganäs, O. Charge Generation in Polymer−Fullerene Bulk-Heterojunction Solar Cells. *Phys. Chem. Chem. Phys.* **2014**, *16*, 20291−20304.

(10) Ohkita, H.; Tamai, Y.; Benten, H.; Ito, S. Transient Absorption Spectroscopy for Polymer Solar Cells. *IEEE J. Sel. Top. Quantum Electron.* **2015**, DOI: 10.1109/JSTQE.2015.2457615.

(11) Yu, G.; Gao, J.; Hummelen, J. C.; Wudl, F.; Heeger, A. J. Polymer Photovoltaic Cells: Enhanced Efficiencies via a Network of Internal Donor-Acceptor Heterojunctions. *Science* **1995**, *270*, 1789−1791.

(12) Halls, J. J. M.; Walsh, C. A.; Greenham, N. C.; Marseglia, E. A.; Friend, R. H.; Moratti, S. C.; Holmes, A. B. Efficient Photodiodes from Interpenetrating Polymer Networks. *Nature* **1995**, *376*, 498−500.

(13) Lakhwani, G.; Rao, A.; Friend, R. H. Bimolecular Recombination in Organic Photovoltaics. *Annu. Rev. Phys. Chem.* **2014**, *65*, 557−581.

(14) Turro, N. J. Energy Transfer. In *Modern Molecular Photochemistry*, 2nd ed.; University Science Books: Sausalito, CA, 1991.

(15) Pope, M.; Swenberg, C. E. *Electronic Processes in Organic Crystals and Polymers*; Oxford University Press: Oxford, U.K., 1999.

(16) Lunt, R. R.; Giebink, N. C.; Belak, A. A.; Benziger, J. B.; Forrest, S. R. Exciton Diffusion Lengths of Organic Semiconductor Thin Films Measured by Spectrally Resolved Photoluminescence Quenching. *J. Appl. Phys.* **2009**, *105*, 053711.

(17) Marciniak, H.; Li, X.-Q.; Würthner, F.; Lochbrunner, S. One-Dimensional Exciton Diffusion in Perylene Bisimide Aggregates. *J. Phys. Chem. A* **2011**, *115*, 648−654.

(18) Lin, J. D. A.; Mikhnenko, O. V.; Chen, J.; Marsi, Z.; Ruseckas, A.; Mikhailovsky, A.; Raab, R. P.; Liu, J.; Blom, P. W. M.; Loi, M. A.; et al. Systematic Study of Exciton Diffusion Length in Organic

Semiconductors by Six Experimental Methods. *Mater. Horiz.* **2014**, *1*, 280−285.

(19) Pettersson, L. A. A.; Roman, L. S.; Inganäs, O. Modeling Photocurrent Action Spectra of Photovoltaic Devices Based on Organic Thin Films. *J. Appl. Phys.* **1999**, *86*, 487−496.

(20) Dicker, G.; de Haas, M. P.; Siebbeles, L. D. A.; Warman, J. M. Electrodeless Time-Resolved Microwave Conductivity Study of Charge-Carrier Photogeneration in Regioregular Poly(3-hexylthiophene) Thin Films. *Phys. Rev. B: Condens. Matter Mater. Phys.* **2004**, *70*, 045203.

(21) Powell, R. C.; Soos, Z. G. Singlet Exciton Energy Transfer in Organic Solids. *J. Lumin.* **1975**, *11*, 1−45.

(22) Yago, T.; Tamaki, Y.; Furube, A.; Katoh, R. Self-Trapping Limited Exciton Diffusion in a Monomeric Perylene Crystal as Revealed by Femtosecond Transient Absorption Microscopy. *Phys. Chem. Chem. Phys.* **2008**, *10*, 4435−4441.

(23) Lunt, R. R.; Benziger, J. B.; Forrest, S. R. Relationship between Crystalline Order and Exciton Diffusion Length in Molecular Organic Semiconductors. *Adv. Mater.* **2010**, *22*, 1233−1236.

(24) Menke, S. M.; Holmes, R. J. Exciton Diffusion in Organic Photovoltaic Cells. *Energy Environ. Sci.* **2014**, *7*, 499−512.

(25) Markov, D. E.; Amsterdam, E.; Blom, P. W. M.; Sieval, A. B.; Hummelen, J. C. Accurate Measurement of the Exciton Diffusion Length in a Conjugated Polymer Using a Heterostructure with a Side-Chain Cross-Linked Fullerene Layer. *J. Phys. Chem. A* **2005**, *109*, 5266−5274.

(26) Markov, D. E.; Tanase, C.; Blom, P. W. M.; Wildeman, J. Simultaneous Enhancement of Charge Transport and Exciton Diffusion in Poly(*p*-phenylene vinylene) Derivatives. *Phys. Rev. B: Condens. Matter Mater. Phys.* **2005**, *72*, 045217.

(27) Markov, D. E.; Blom, P. W. M. Anisotropy of Exciton Migration in Poly(*p*-phenylene vinylene). *Phys. Rev. B: Condens. Matter Mater. Phys.* **2006**, *74*, 085206.

(28) Scully, S. R.; McGehee, M. D. Effects of Optical Interference and Energy Transfer on Exciton Diffusion Length Measurements in Organic Semiconductors. *J. Appl. Phys.* **2006**, *100*, 034907.

(29) Mikhnenko, O. V.; Cordella, F.; Sieval, A. B.; Hummelen, J. C.; Blom, P. W. M.; Loi, M. A. Temperature Dependence of Exciton Diffusion in Conjugated Polymers. *J. Phys. Chem. B* **2008**, *112*, 11601−11604.

(30) Goh, C.; Scully, S. R.; McGehee, M. D. Effects of Molecular Interface Modification in Hybrid Organic-Inorganic Photovoltaic Cells. *J. Appl. Phys.* **2007**, *101*, 114503.

(31) Huijser, A.; Savenije, T. J.; Shalav, A.; Siebbeles, L. D. A. An Experimental Study on the Molecular Organization and Exciton Diffusion in a Bilayer of a Porphyrin and Poly(3-hexylthiophene). *J. Appl. Phys.* **2008**, *104*, 034505.

(32) Shaw, P. E.; Ruseckas, A.; Samuel, I. D. W. Exciton Diffusion Measurements in Poly(3-hexylthiophene). *Adv. Mater.* **2008**, *20*, 3516−3520.

(33) Wang, Y.; Benten, H.; Ohara, S.; Kawamura, D.; Ohkita, H.; Ito, S. Measurement of Exciton Diffusion in a Well-Defined Donor/Acceptor Heterojunction Based on a Conjugated Polymer and Cross-Linked Fullerene Derivative. *ACS Appl. Mater. Interfaces* **2014**, *6*, 14108−14115.

(34) Mikhnenko, O. V.; Azimi, H.; Scharber, M.; Morana, M.; Blom, P. W. M.; Loi, M. A. Exciton Diffusion Length in Narrow Bandgap Polymers. *Energy Environ. Sci.* **2012**, *5*, 6960−6965.

(35) Mikhnenko, O. V.; Kuik, M.; Lin, J.; van der Kaap, N.; Nguyen, T.-Q.; Blom, P. W. M. Trap-Limited Exciton Diffusion in Organic Semiconductors. *Adv. Mater.* **2014**, *26*, 1912−1917.

(36) Bruno, A.; Reynolds, L. X.; Dyer-Smith, C.; Nelson, J.; Haque, S. A. Determining the Exciton Diffusion Length in a Polyfluorene from Ultrafast Fluorescence Measurements of Polymer/Fullerene Blend Films. *J. Phys. Chem. C* **2013**, *117*, 19832−19838.

(37) Collins, B. A.; Gann, E.; Guignard, L.; He, X.; McNeill, C. R.; Ade, H. Molecular Miscibility of Polymer−Fullerene Blends. *J. Phys. Chem. Lett.* **2010**, *1*, 3160−3166.

(38) Treat, N. D.; Brady, M. A.; Smith, G.; Toney, M. F.; Kramer, E. J.; Hawker, C. J.; Chabinyc, M. L. Interdiffusion of PCBM and P3HT Reveals Miscibility in a Photovoltaically Active Blend. *Adv. Energy Mater.* **2011**, *1*, 82−89.

(39) Cook, S.; Liyuan, H.; Furube, A.; Katoh, R. Singlet Annihilation in Films of Regioregular Poly(3-hexylthiophene): Estimates for Singlet Diffusion Lengths and the Correlation between Singlet Annihilation Rates and Spectral Relaxation. *J. Phys. Chem. C* **2010**, *114*, 10962−10968.

(40) Engel, E.; Leo, K.; Hoffmann, M. Ultrafast Relaxation and Exciton−Exciton Annihilation in PTCDA Thin Films at High Excitation Densities. *Chem. Phys.* **2006**, *325*, 170−177.

(41) Tamai, Y.; Matsuura, Y.; Ohkita, H.; Benten, H.; Ito, S. One-Dimensional Singlet Exciton Diffusion in Poly(3-hexylthiophene) Crystalline Domains. *J. Phys. Chem. Lett.* **2014**, *5*, 399−403.

(42) Razi Naqvi, K. Diffusion-Controlled Reactions in Two-Dimensional Fluids: Discussion of Measurements of Lateral Diffusion of Lipids in Biological Membranes. *Chem. Phys. Lett.* **1974**, *28*, 280−284.

(43) Yamanaka, K.; Okada, T.; Goto, Y.; Tani, T.; Inagaki, S. Exciton Migration Dynamics between Phenylene Moieties in the Framework of Periodic Mesoporous Organosilica Powder. *RSC Adv.* **2013**, *3*, 14774−14779.

(44) Masuda, K.; Ikeda, Y.; Ogawa, M.; Benten, H.; Ohkita, H.; Ito, S. Exciton Generation and Diffusion in Multilayered Organic Solar Cells Designed by Layer-by-Layer Assembly of Poly(*p*-phenylenevinylene). *ACS Appl. Mater. Interfaces* **2010**, *2*, 236−245.

(45) Laquai, F.; Park, Y.-S.; Kim, J.-J.; Basché, T. Excitation Energy Transfer in Organic Materials: From Fundamentals to Optoelectronic Devices. *Macromol. Rapid Commun.* **2009**, *30*, 1203−1231.

(46) Hwang, I.; Scholes, G. D. Electronic Energy Transfer and Quantum-Coherence in π-Conjugated Polymers. *Chem. Mater.* **2011**, *23*, 610−620.

(47) Hennebicq, E.; Pourtois, G.; Scholes, G. D.; Herz, L. M.; Russell, D. M.; Silva, C.; Setayesh, S.; Grimsdale, A. C.; Müllen, K.; Brédas, J.-L.; et al. Exciton Migration in Rigid-Rod Conjugated Polymers: An Improved Förster Model. *J. Am. Chem. Soc.* **2005**, *127*, 4744−4762.

(48) Van Averbeke, B.; Beljonne, D.; Hennebicq, E. Energy Transport along Conjugated Polymer Chains: Through-Space or Through-Bond? *Adv. Funct. Mater.* **2008**, *18*, 492−498.

(49) Shekhar, S.; Aharon, E.; Tian, N.; Galbrecht, F.; Scherf, U.; Holder, E.; Frey, G. L. Decoupling 2D Inter- and Intrachain Energy Transfer in Conjugated Polymers. *ChemPhysChem* **2009**, *10*, 576−581.

(50) Kroeze, J. E.; Savenije, T. J.; Vermeulen, M. J. W.; Warman, J. M. Contactless Determination of the Photoconductivity Action Spectrum, Exciton Diffusion Length, and Charge Separation Efficiency in Polythiophene-Sensitized TiO₂ Bilayers. *J. Phys. Chem. B* **2003**, *107*, 7696−7705.

(51) Lüer, L.; Egelhaaf, H.-J.; Oelkrug, D.; Cerullo, G.; Lanzani, G.; Huisman, B.-H.; de Leeuw, D. Oxygen-Induced Quenching of Photoexcited States in Polythiophene Films. *Org. Electron.* **2004**, *5*, 83−89.

(52) Spano, F. C. Modeling Disorder in Polymer Aggregates: The Optical Spectroscopy of Regioregular Poly(3-hexylthiophene) Thin Films. *J. Chem. Phys.* **2005**, *122*, 234701.

(53) Spano, F. C. Absorption in Regio-Regular Poly(3-hexyl)-thiophene Thin Films: Fermi Resonaces, Interband Coupling and Disorder. *Chem. Phys.* **2006**, *325*, 22−35.

(54) Clark, J.; Chang, J.-F.; Spano, F. C.; Friend, R. H.; Silva, C. Determining Exciton Bandwidth and Film Microstructure in Polythiophene Films using Linear Absorption Spectroscopy. *Appl. Phys. Lett.* **2009**, *94*, 163306.

(55) Yang, X.; Loos, J.; Veenstra, S. C.; Verhees, W. J. H.; Wienk, M. M.; Kroon, J. M.; Michels, M. A. J.; Janssen, R. A. J. Nanoscale Morphology of High-Performance Polymer Solar Cells. *Nano Lett.* **2005**, *5*, 579−583.

(56) van Bavel, S. S.; Bärenklau, M.; de With, G.; Hoppe, H.; Loos, J. P3HT/PCBM Bulk Heterojunction Solar Cells: Impact of Blend

Composition and 3D Morphology on Device Performance. *Adv. Funct. Mater.* **2010**, *20*, 1458–1463.

(57) Lim, J. A.; Liu, F.; Ferdous, S.; Muthukumar, M.; Briseno, A. L. Polymer Semiconductor Crystals. *Mater. Today* **2010**, *13*, 14–24.

(58) Köse, M. E. Evaluation of Excitonic Coupling and Charge Transport Integrals in P3HT Nanocrystal. *J. Phys. Chem. C* **2011**, *115*, 13076–13082.

(59) Spano, F. C.; Clark, J.; Silva, C.; Friend, R. H. Determining Exciton Coherence from the Photoluminescence Spectral Line Shape in Poly(3-hexylthiophene) Thin Films. *J. Chem. Phys.* **2009**, *130*, 074904.

(60) Zhang, X.; Li, Z.; Lu, G. First-Principles Simulations of Exciton Diffusion in Organic Semiconductors. *Phys. Rev. B: Condens. Matter Mater. Phys.* **2011**, *84*, 235208.

(61) Bjorgaard, J. A.; Köse, M. E. Simulations of Exciton Diffusion and Trapping in Semicrystalline Morphologies of Poly(3-hexylthiophene). *J. Phys. Chem. C* **2014**, *118*, 5576–5761.

(62) Bjorgaard, J. A.; Köse, M. E. Simulations of Singlet Exciton Diffusion in Organic Semiconductors: A Review. *RSC Adv.* **2015**, *5*, 8432–8445.

(63) Guo, J.; Ohkita, H.; Benten, H.; Ito, S. Charge Generation and Recombination Dynamics in Poly(3-hexylthiophene)/Fullerene Blend Films with Different Regioregularities and Morphologies. *J. Am. Chem. Soc.* **2010**, *132*, 6154–6164.

(64) Yamamoto, S.; Ohkita, H.; Benten, H.; Ito, S. Role of Interfacial Charge Transfer State in Charge Generation and Recombination in Low-Bandgap Polymer Solar Cell. *J. Phys. Chem. C* **2012**, *116*, 14804–14810.

(65) Tamai, Y.; Tsuda, K.; Ohkita, H.; Benten, H.; Ito, S. Charge-Carrier Generation in Organic Solar Cells Using Crystalline Donor Polymers. *Phys. Chem. Chem. Phys.* **2014**, *16*, 20338–20346.

(66) Credgington, D.; Durrant, J. R. Insights from Transient Optoelectronic Analyses on the Open-Circuit Voltage of Organic Solar Cells. *J. Phys. Chem. Lett.* **2012**, *3*, 1465–1478.

(67) Guo, X.; Zhou, N.; Lou, S. J.; Smith, J.; Tice, D. B.; Hennek, J. W.; Ortiz, R. P.; Navarrete, J. T. L.; Li, S.; Strzalka, J.; et al. Polymer Solar Cells with Enhanced Fill Factors. *Nat. Photonics* **2013**, *7*, 825–833.

(68) Li, W.; Hendriks, K. H.; Roelofs, W. S. C.; Kim, Y.; Wienk, M. M.; Janssen, R. A. J. Efficient Small Bandgap Polymer Solar Cells with High Fill Factors for 300 nm Thick Films. *Adv. Mater.* **2013**, *25*, 3182–3186.

(69) Osaka, I.; Saito, M.; Koganezawa, T.; Takimiya, K. Thiophene–Thiazolothiazole Copolymers: Significant Impact of Side Chain Composition on Backbone Orientation and Solar Cell Performances. *Adv. Mater.* **2014**, *26*, 331–338.

(70) Vohra, V.; Kawashima, K.; Kakara, T.; Koganezawa, T.; Osaka, I.; Takimiya, K.; Murata, H. Efficient Inverted Polymer Solar Cells Employing Favourable Molecular Orientation. *Nat. Photonics* **2015**, *9*, 403–408.

(71) Jamieson, F. C.; Domingo, E. B.; McCarthy-Ward, T.; Heeney, M.; Stingelin, N.; Durrant, J. R. Fullerene Crystallisation as a Key Driver of Charge Separation in Polymer/Fullerene Bulk Heterojunction Solar Cells. *Chem. Sci.* **2012**, *3*, 485–492.

(72) Li, W.; Hendriks, K. H.; Furlan, A.; Roelofs, W. S. C.; Wienk, M. M.; Janssen, R. A. J. Universal Correlation between Fibril Width and Quantum Efficiency in Diketopyrrolopyrrole-Based Polymer Solar Cells. *J. Am. Chem. Soc.* **2013**, *135*, 18942–18948.

(73) Li, Z.; Lin, J. D. A.; Phan, H.; Sharenko, A.; Proctor, C. M.; Zalar, P.; Chen, Z.; Facchetti, A.; Nguyen, T.-Q. Competitive Absorption and Inefficient Exciton Harvesting: Lessons Learned from Bulk Heterojunction Organic Photovoltaics Utilizing the Polymer Acceptor P(NDI2OD-T2). *Adv. Funct. Mater.* **2014**, *24*, 6989–6998.

(74) Albert-Seifried, S.; Ko, D.-H.; Hüttner, S.; Kanimozhi, C.; Patil, S.; Friend, R. H. Efficiency Limitations in a Low Band-Gap Diketopyrrolopyrrole-Based Polymer Solar Cell. *Phys. Chem. Chem. Phys.* **2014**, *16*, 6743–6752.

(75) Mani, A.; Schoonman, J.; Goossens, A. Photoluminescence Study of Sexithiophene Thin Films. *J. Phys. Chem. B* **2005**, *109*, 4829–4836.

(76) Kurrle, D.; Pflaum, J. Exciton Diffusion Length in the Organic Semiconductor Diindenoperylene. *Appl. Phys. Lett.* **2008**, *92*, 133306.

(77) Marciniak, H.; Li, X.-Q.; Würthner, F.; Lochbrunner, S. One-Dimensional Exciton Diffusion in Perylene Bisimide Aggregates. *J. Phys. Chem. A* **2011**, *115*, 648–654.

(78) Paquin, F.; Yamagata, H.; Hestand, N. J.; Sakowicz, M.; Bérubé, N.; Côté, M.; Reynolds, L. X.; Haque, S. A.; Stingelin, N.; Spano, F. C.; et al. Two-Dimensional Spatial Coherence of Excitons in Semicrystalline Polymeric Semiconductors: Effect of Molecular Weight. *Phys. Rev. B: Condens. Matter Mater. Phys.* **2013**, *88*, 155202.

(79) Kuhn, H. Classical Aspects of Energy Transfer in Molecular Systems. *J. Chem. Phys.* **1970**, *53*, 101–108.

(80) Chance, R. R.; Prock, A.; Silbey, R. Molecular Fluorescence and Energy Transfer Near Interfaces. In *Advances in Chemical Physics*, Vol. 37; John Wiley & Sons, Inc.: Hoboken, NJ, 1978.

(81) Scully, S. R.; Armstrong, P. B.; Edder, C.; Fréchet, J. M. J.; McGehee, M. D. Long-Range Resonant Energy Transfer for Enhanced Exciton Harvesting for Organic Solar Cells. *Adv. Mater.* **2007**, *19*, 2961–2966.

(82) Wang, Y.; Ohkita, H.; Benten, H.; Ito, S. Efficient Exciton Harvesting through Long-Range Energy Transfer. *ChemPhysChem* **2015**, *16*, 1263–1267.

(83) Honda, S.; Nogami, T.; Ohkita, H.; Benten, H.; Ito, S. Improvement of the Light-Harvesting Efficiency in Polymer/Fullerene Bulk Heterojunction Solar Cells by Interfacial Dye Modification. *ACS Appl. Mater. Interfaces* **2009**, *1*, 804–810.

(84) Honda, S.; Ohkita, H.; Benten, H.; Ito, S. Selective Dye Loading at the Heterojunction in Polymer/Fullerene Solar Cells. *Adv. Energy Mater.* **2011**, *1*, 588–598.

(85) Honda, S.; Yokoya, S.; Ohkita, H.; Benten, H.; Ito, S. Light-Harvesting Mechanism in Polymer/Fullerene/Dye Ternary Blends Studied by Transient Absorption Spectroscopy. *J. Phys. Chem. C* **2011**, *115*, 11306–11317.

(86) Xu, H.; Ohkita, H.; Hirata, T.; Benten, H.; Ito, S. Near-IR Dye Sensitization of Polymer Blend Solar Cells. *Polymer* **2014**, *55*, 2856–2860.

(87) Xu, H.; Ohkita, H.; Tamai, Y.; Benten, H.; Ito, S. Interface Engineering for Ternary Blend Polymer Solar Cells with Hetero-structured Near-IR Dye. *Adv. Mater.* **2015**, DOI: 10.1002/adma.201502773.

(88) Koppe, M.; Egelhaaf, H.-J.; Clodic, E.; Morana, M.; Lüer, L.; Troeger, A.; Sgobba, V.; Guldi, D. M.; Ameri, T.; Brabec, C. J. Charge Carrier Dynamics in a Ternary Bulk Heterojunction System Consisting of P3HT, Fullerene, and a Low Bandgap Polymer. *Adv. Energy Mater.* **2013**, *3*, 949–958.

(89) Fushimi, T.; Oda, A.; Ohkita, H.; Ito, S. Triplet Energy Migration in Layer-by-Layer Deposited Ultrathin Polymer Films Bearing Tris(2,2′-bipyridine)ruthenium(II) Moieties. *J. Phys. Chem. B* **2004**, *108*, 18897–18902.

(90) Samiullah, M.; Moghe, D.; Scherf, U.; Guha, S. Diffusion Length of Triplet Excitons in Organic Semiconductors. *Phys. Rev. B: Condens. Matter Mater. Phys.* **2010**, *82*, 205211.

(91) Wallikewitz, B. H.; Kabra, D.; Gélinas, S.; Friend, R. H. Triplet Dynamics in Fluorescent Polymer Light-Emitting Diodes. *Phys. Rev. B: Condens. Matter Mater. Phys.* **2012**, *85*, 045209.

(92) Tamai, Y.; Ohkita, H.; Benten, H.; Ito, S. Triplet Exciton Dynamics in Fluorene–Amine Copolymer Films. *Chem. Mater.* **2014**, *26*, 2733–2742.

(93) Najafov, H.; Lee, B.; Zhou, Q.; Feldman, L. C.; Podzorov, V. Observation of Long-Range Exciton Diffusion in Highly Ordered Organic Semiconductors. *Nat. Mater.* **2010**, *9*, 938–943.

(94) Kraabel, B.; Moses, D.; Heeger, A. J. Direct Observation of the Intersystem Crossing in Poly(3-hexylthiophene). *J. Chem. Phys.* **1995**, *103*, 5102–5108.

(95) Smith, M. B.; Michl, J. Singlet Fission. *Chem. Rev.* **2010**, *110*, 6891–6936.

(96) Smith, M. B.; Michl, J. Recent Advances in Singlet Fission. *Annu. Rev. Phys. Chem.* **2013**, *64*, 361−386.

(97) Hanna, M. C.; Nozik, A. J. Solar Conversion Efficiency of Photovoltaic and Photoelectrolysis Cells with Carrier Multiplication Absorbers. *J. Appl. Phys.* **2006**, *100*, 074510.

(98) Nozik, A. J. Multiple Exciton Generation in Semiconductor Quantum Dots. *Chem. Phys. Lett.* **2008**, *457*, 3−11.

(99) Rao, A.; Wilson, M. W. B.; Albert-Seifried, S.; Di Pietro, R.; Friend, R. H. Photophysics of Pentacene Thin Films: The Role of Exciton Fission and Heating Effects. *Phys. Rev. B: Condens. Matter Mater. Phys.* **2011**, *84*, 195411.

(100) Ma, L.; Zhang, K.; Kloc, C.; Sun, H.; Michel-Beyerle, M. E.; Gurzadyan, G. G. Singlet Fission in Rubrene Single Crystal: Direct Observation by Femtosecond Pump−Probe Spectroscopy. *Phys. Chem. Chem. Phys.* **2012**, *14*, 8307−8312.

(101) Piland, G. B.; Burdett, J. J.; Kurunthu, D.; Bardeen, C. J. Magnetic Field Effects on Singlet Fission and Fluorescence Decay Dynamics in Amorphous Rubrene. *J. Phys. Chem. C* **2013**, *117*, 1224−1236.

(102) Yost, S. R.; Lee, J.; Wilson, M. W. B.; Wu, T.; McMahon, D. P.; Parkhurst, R. R.; Thompson, N. J.; Congreve, D. N.; Rao, A.; Johnson, K.; et al. A Transferable Model for Singlet-Fission Kinetics. *Nat. Chem.* **2014**, *6*, 492−497.

(103) Wohlgenannt, M.; Graupner, W.; Leising, G.; Vardeny, Z. V. Photogeneration and Recombination Processes of Neutral and Charged Excitations in Films of a Ladder-Type Poly(*para*-phenylene). *Phys. Rev. B: Condens. Matter Mater. Phys.* **1999**, *60*, 5321−5330.

(104) Österbacka, R.; Wohlgenannt, M.; Shkunov, M.; Chinn, D.; Vardeny, Z. V. Excitons, Polarons, and Laser Action in Poly(*p*-phenylene vinylene) Films. *J. Chem. Phys.* **2003**, *118*, 8905−8916.

(105) Guo, J.; Ohkita, H.; Benten, H.; Ito, S. Near-IR Femtosecond Transient Absorption Spectroscopy of Ultrafast Polaron and Triplet Exciton Formation in Polythiophene Films with Different Regioregularities. *J. Am. Chem. Soc.* **2009**, *131*, 16869−16880.

(106) Tamai, Y.; Ohkita, H.; Benten, H.; Ito, S. Singlet Fission in Poly(9,9′-di-*n*-octylfluorene) Films. *J. Phys. Chem. C* **2013**, *117*, 10277−10284.

(107) Musser, A. J.; Al-Hashimi, M.; Maiuri, M.; Brida, D.; Heeney, M.; Cerullo, G.; Friend, R. H.; Clark, J. Activated Singlet Exciton Fission in a Semiconducting Polymer. *J. Am. Chem. Soc.* **2013**, *135*, 12747−12754.

(108) Busby, E.; Xia, J.; Wu, Q.; Low, J. Z.; Song, R.; Miller, J. R.; Zhu, X.-Y.; Campos, L. M.; Sfeir, M. Y. A Design Strategy for Intramolecular Singlet Fission Mediated by Charge-Transfer States in Donor−Acceptor Organic Materials. *Nat. Mater.* **2015**, *14*, 426−433.